ChemComm

RSC Publishing

COMMUNICATION

View Article Online
View Journal | View Issue

Cite this: *Chem. Commun.*, 2013, **49**, 6876

Received 5th April 2013,
Accepted 10th June 2013

DOI: 10.1039/c3cc42475h

www.rsc.org/chemcomm

Synthesis of heterogeneous enzyme–metal nanoparticle biohybrids in aqueous media and their applications in C–C bond formation and tandem catalysis†

Marco Filice,*[a] Marzia Marciello,[b] Maria del Puerto Morales[b] and Jose M. Palomo*[a]

The straightforward synthesis of novel enzyme–metalNP nanobiohybrids in aqueous medium was developed. These new nanobiohybrids were excellent multivalent catalysts combining both activities in various sets of synthetic reactions even at ultra-low concentrations (ppb amount).

Nanocatalysts have undergone explosive growth during the past decade, both in homogeneous and heterogeneous forms.[1,2] The large surface-to-volume ratio of nanomaterials compared to bulk materials makes them attractive candidates for their application as catalysts.[3] For example, palladium nanoparticles (PdNPs) have played a pivotal role in a wide variety of C–C coupling reactions.[4] Generally, the most useful approaches for synthesis of nanoparticles[5] usually employ harsh conditions. Therefore, biological methods could represent a green alternative. For example, RNA sequences or polypeptides were discovered to aid the formation of nanoparticles by using a reducing agent (typically ascorbic acid or sodium borohydride).[6–7] Amongst all the biomacromolecules, enzymes are natural proteins with nanodimensions (*e.g.*, lipase from *Candida antarctica* B; 3 nm × 4 nm × 5 nm) that can catalyse a wide set of reactions with exquisite control of regio- and stereochemistry. They have also been involved as reactants in the synthesis of metal nanoparticles[8] and hybrid nanostructures.[9]

Therefore, considering the continuous demand for the development of new catalysts with high-efficiency and a broad reaction scope, the creation of heterogeneous hybrid nanocatalysts with an overall catalytic activity resulting from the combination of two different but complementary catalytic activities (noble metal NPs together with enzymes) could represent a straightforward breakthrough in this field.

Here we describe the synthesis of novel enzyme–metalNP nanobiohybrids, where NPs were generated *in situ* from an aqueous noble metal salt solution (Scheme 1). The enzyme acted as a (i) reducing agent for nanoparticle formation, (ii) a stabilizing and supporting agent (avoiding nanoparticle aggregation) and (iii) a biocatalyst, all at the same time. These new nanobiohybrids were successfully applied as heterogeneous catalysts in a set of different interesting reactions exploiting selectively the catalytic activity of the metal, the enzyme or both at the same time (domino and tandem reactions). Furthermore, these new catalysts were recycled several times keeping their catalytic properties intact. Initially, the synthesis of the nanobiohybrids in aqueous medium was attempted by adding the commercial liquid *Candida antarctica B* lipase (CAL-B) to an aqueous solution of fully water soluble Na_2PdCl_4 salt at room temperature and under gentle stirring. After 24 h, the initial clear solution turned into a slight cloudy suspension where only 10% of the enzyme disappeared (by the Bradford method[10]) forming a heterogeneous composite (Table 1 and Table S1, ESI†).

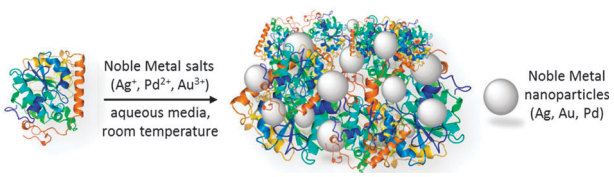

Scheme 1 Preparation strategy for enzyme–metalNP biohybrids.

Using $Pd(OAc)_2$ in the presence of different co-solvents, a quantitative precipitation of the protein was observed after 24 h (Table 1). An ICP-AES analysis of the supernatants revealed that 6.45–7.57 μmol of Pd^{2+} were entrapped into the protein. CALB–PdNP-(2–7) biohybrids were recovered by centrifugation, washed with distilled water and lyophilized.

TGA of the CALB–PdNPs-2 lyophilized powder (Fig. S1, ESI†) showed that 26% (w/w) of the amount of Pd comprised the solid material, confirming the value previously obtained using ICP-AES.

As an initial representative example, the CALB–PdNPs-2 nanobiohybrid was fully characterized using SEM, EDX, XRD, XPS and TEM (Fig. 1 and Fig. S2, ESI†). The EDX experiment (Fig. 1) as well as SEM analysis revealed that the formed precipitate was composed of an aggregate with a mesoporous amorphous suprastructure composed of palladium atoms dispersed into an organic matrix (CAL-B) (Fig. S2a, ESI†). TEM analysis together with XRD and XPS

[a] *Departamento de Biocatálisis, Instituto de Catálisis (ICP-CSIC), Marie Curie 2, Cantoblanco, Campus UAM, 28049 Madrid, Spain. E-mail: marcof@icp.csic.es, josempalomo@icp.csic.es*

[b] *Departamento de Biomateriales y Materiales Bioinspirados, Instituto de Ciencia de Materiales, (ICMM-CSIC), Sor Juana Inés de la Cruz 3, Campus UAM, 28049 Madrid, Spain*

† Electronic supplementary information (ESI) available: Experimental section, characterization data of the different nanobiohybrids, recycling studies and additional tables and figures. See DOI: 10.1039/c3cc42475h

Table 1 Synthesis of enzyme–Pd nanobiohybrids

Catalyst	Co-solvent[a]	Metal salt (1 mg mL^{-1})	Protein amount[b] (%)	Metal amount[c] (μmol)
CALB–PdNPs-1	—	Na_2PdCl_4	10	nd
CALB–PdNPs-2	DMF	$Pd(OAc)_2$	99	6.45
CALB–PdNPs-4	ACN	$Pd(OAc)_2$	99	7
CALB–PdNPs-5	MeOH	$Pd(OAc)_2$	99	6.68
CALB–PdNPs-6	THF	$Pd(OAc)_2$	99	7.12

[a] 20% (v/v). [b] Calculated by the Bradford assay of the supernatant after 24 h. [c] Calculated using ICP-AES analysis of the supernatant after 24 h.

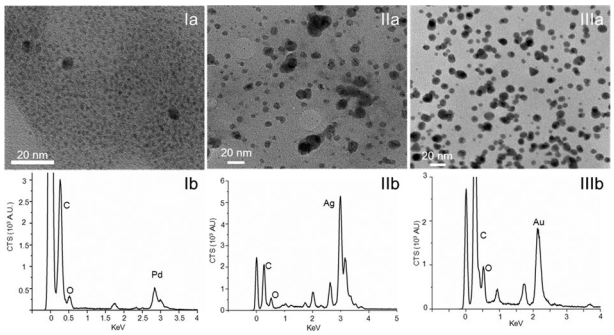

Fig. 1 Physicochemical characterization of nanobiohybrids (I) CALB–PdNPs-2, (II) CALB–AgNPs-1, (III) CALB–AuNPs-1 and (a) TEM images. (b) EDX pattern.

experiments (Fig. S2, ESI†) confirmed the generation of PdNPs embedded in the protein net (Fig. 1). The morphology and the distribution of PdNPs were investigated using TEM and HRTEM. A dual particle size distribution was observed (Fig. 1 and Fig. S2, ESI†). The main fraction was composed of rather spherical particles with an average diameter of 1.3 nm densely deposited throughout the hybrid composite. The minor fraction was composed of larger NPs with an average diameter of 4.5 nm randomly decorating the enzymatic network (Fig. S2, ESI†). The HRTEM image of the larger NPs clearly showed their atomic lattice, confirming the high crystallinity of the NPs (Fig. S2, ESI†). The CALB–PdNP (3–6) biohybrids were also characterized using EDX and TEM (Fig. S3, ESI†). In all the cases, the bimodal distribution in NPs was maintained although with slight differences in distribution size (1.5–3.5 and 5.5–6.8 nm average size for main smaller NPs and minor larger NPs, respectively (Fig. S3, ESI†)).

To expand the method, $AgNO_3$ and $HAuCl_4$ were tested as precursors with the same experimental procedure previously developed for CALB–PdNPs hybrids. Under the best conditions, quantitative (CALB–AgNPs-2) or almost quantitative (CALB–AuNPs-1) yields of both biohybrids were achieved (Table S2, ESI†). ICP analysis revealed that 37–41 μmol of Ag^+ and about 19 μmol of Au^{3+} were entrapped inside the protein net. EDX and TEM analyses confirmed the presence of silver or gold spherical nanoparticles (Fig. 1 and Fig. S4, ESI†) with a unique particle size distribution of about 8 nm average diameter for CALB–AgNPs-1 and CALB–AuNPs-1, and 10 nm for CALB–AgNPs-2 and CALB–AuNPs-2 (Fig. S4, ESI†).

Therefore, considering all these results, a two-step mechanism for the enzyme–noble metal NPs nanobiohybrid formation can be proposed (Scheme S1, ESI†): (i) a first rapid adsorption of soluble Me^{n+} ions on the enzyme, reducing its solubility and acting as a cross-linker between the enzyme molecules (initial fast precipitation) and afterwards, (ii) an "*in situ*" reduction of metal ions in the absence of any exogenous reducing agents, finally generating the NPs.[11–12] FTIR experiments together with the pH-dependent zeta potential measurement of native CAL-B and the CALB–PdNPs-2, supported this idea (Fig. S5, ESI†) (For a more detailed discussion on the nanobiohybrid formation mechanism, see ESI†).

The synthesized metal NPs were very stable in aqueous solution without any changes in particle size and morphology for three months (data not shown) providing further evidence that the enzyme network acts not only as a physical support and reducing agent during the NP synthesis but also serves as a stabilizing agent.

The catalytic properties of CALB–metalNP biohybrids were initially tested in the hydrolysis of 4-nitrophenyl butyrate **1** to obtain the chromogenic 4-nitrophenol **2** (by enzyme catalysis), in the reduction of **2** to 4-aminophenol **3** (by metal catalysis) and in the domino one-pot transformation of **1** to **3** (by combo-catalysis) as model reactions (Fig. 2 and Table S3, ESI†).

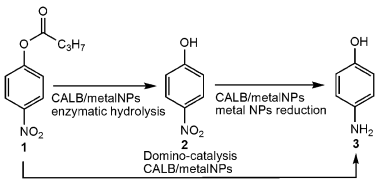

Fig. 2 Domino reaction for the synthesis of aminoarene **3**.

Among all the Pd nanohybrids, CALB–PdNPs-5 and CALB–PdNPs-6 recovered the highest enzymatic activity (around 47%) in the hydrolysis of **1** compared to the starting soluble CALB. Almost no enzymatic activity (<5%) was found in the CALB–AgNP biohybrids, whereas 25% of the initial enzymatic activity was recovered in the CALB–AuNP biohybrids (Table S3, ESI†). For the catalytic reduction of **2**, the reaction rate constant (k) and the turnover frequency number (TOF) for the CALB–metalNP biohybrids were calculated, showing better enzymatic activity (Table S3, Fig. S6–S8, ESI†). The CALB–PdNPs-5 biohybrid exhibited the highest k and TOF values (0.6 min^{-1} and almost 150 min^{-1}, respectively) with only slight differences compared to CALB–PdNPs-6 (Table S3, ESI†). As far as we know, the TOF value is *the highest* described in the literature for this reaction.[13] k and TOF values for CALB–AgNPs-1 and CALB–AuNPs-1 were 0.28 min^{-1} and about 10 min^{-1}, and 0.31 min^{-1} and about 28 min^{-1}, respectively, these values being comparable to the best ones reported in the literature for these metals.[14] Consequently, CALB–PdNPs-5 was selected for the direct domino transformation of **1** to **3** (Fig. 2 and Fig. S6, ESI†) confirming the good results previously achieved for separate.

We continued our study evaluating the catalytic performance of the CALB–PdNPs in C–C coupling reactions. The Suzuki–Miyaura cross coupling reaction in aqueous media was attempted using the CALB–PdNPs-2 biohybrid as the catalyst (considering the high surface area of NPs owing to their small average diameter and highest catalytic activity in the reduction of **2**) (Table 2). Different aryl-halides, bases and phase transfer catalysts (PTC)[15] were evaluated (Table 2 and Table S4, ESI†).

Upon using chlorobenzene, the reaction yield was negligible in all the cases (Table 2, entry 1), whereas a 50–55% yield of biphenyl **6** was obtained when aryl-bromide or iodide was used (Table 2, entries 2 and 3). The addition of PTCs showed a positive effect only when the reaction was performed in the

Table 2 Suzuki-Miyaura coupling catalyzed by CALB–PdNPs-2[a]

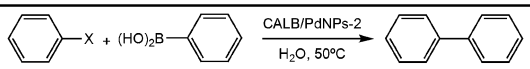

4 5 6

Entry	X	PTC[b]	Base[c]	Time (h)	Yield[d] (%)
1	Cl	—	NaOH	48	2
2	Br	—	NaOH	24	50
3	I	—	NaOH	24	55
4	Br	TBACl	NaOH	2.5	99
5	I	TBACl	NaOH	38	52

[a] Reaction conditions: **4** (0.5 mmol), **5** (0.55 mmol), H_2O (1 mL), 130 ppb of Pd catalyst, 50 °C. [b] Phase transfer catalyst; 0.165 mmol. [c] 1.5 eq. [d] Calculated by HPLC analysis as described in the ESI.

Table 3 Heck coupling catalyzed by CALB–PdNPs-4[a]

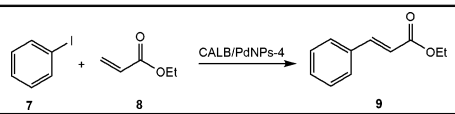

7 8 9

Co-solvent (%v/v, H_2O)	T (°C)	Time (h)	Yield[b] (%)
—	70	24	0
25	70	18	99
50	70	24	20

[a] Reaction conditions: **7** (0.274 mmol), **8** (0.55 mmol), DMF (1 mL), 1 mg of CALB–PdNPs-4 catalyst, 70 °C, triethylamine (TEA) (0.412 mmol). [b] Calculated by HPLC analysis as described in the ESI.

presence of aryl-bromide achieving almost quantitative yields of **6** in the presence of TBACl (Table 2, entry 4), using 0.025% (mol/mol) of Pd (about 130 ppb of Pd), with a TON and TOF of 3876 and 1550 h^{-1}, respectively.[16] The nanobiohybrid was used for 5 reaction cycles retrieving similar results (in terms of yield and rate (TOF)) in each cycle and without significant loss of activity (Table S5, ESI†).

To further expand the practical application of these biohybrids in organic synthesis, the Heck reaction was studied (Table 3 and Table S6, ESI†) selecting CALB–PdNPs-4 as the representative catalyst.

Different reaction parameters, such as temperature or presence of water, were evaluated in order to soften the common harsh reaction conditions (Table S6, ESI†). Under the best conditions, quantitative yield of product **9** was achieved in 18 h at 70 °C with 25% (v/v) water (Table 3). The biohybrids CALB–PdNPs-2, 5 and 6 exhibited similar results (data not shown).

Table 4 DKR of **10** catalyzed by CALB–PdNPs-5[a]

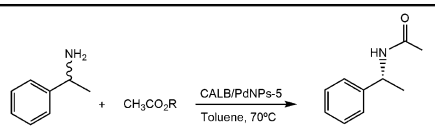

(±)-10 (R)-13

Entry	R	Base[b]	Time (h)	C[c] (%)	ee[d] (%)
1	$Prop_{iso}$	—	5	88	90
2	Et	—	4	98	>99
3	Et	TEA	4	91	28
4[e]	Et		4	98	>99

[a] Reaction conditions: **10** (0.01 mmol), **11** or **12** (0.06 mmol), toluene (1 mL) and 70 °C, 5 mg CALB–PdNPs-5. [b] 0.07 mmol. [c] Calculated by RP-HPLC analysis. [d] Determined by chiral HPLC. [e] CALB–PdNPs-6 was used as the catalyst.

Finally, the nanocatalysts were tested in a tandem catalysis process (both enzymatic and Pd catalytic activities at the same time) for the dynamic kinetic resolution (DKR) of *rac*-phenylethylamine **10** (Table 4 and Table S7, ESI†).

Firstly, both reactions (hydrolysis and racemization) were studied separately (Fig. S9, ESI†). Free lyophilized CALB was used to study the enzymatic transesterification of **10**, showing a very high enantioselectivity toward the *R* enantiomer (ee > 99%). The CALB–PdNPs-4 and CALB–PdNPs-5 were used in the Pd-racemization process of the enantiopure *S*-**10** achieving the *rac*-**10** in both cases (Table S8, ESI†). Therefore, the tandem enzyme–Pd catalysis was performed using CALB–PdNPs-5 which was the best catalyst in terms of enzymatic hydrolytic activity. Different parameters such as acyl donors, use of molecular sieves or different bases were evaluated (Table 4, Table S7, ESI†). In the best case, using ethylacetate as the acylating agent, *rac*-**10** was transformed by CALB–PdNPs-5 into *R*-**13** in almost quantitative yield and excellent enantiopurity (ee > 99%) in 4 h. The CALB–PdNPs-5 was reused for three cycles maintaining its activity and selectivity intact (Table S9, ESI†). Under the same conditions, the CALB–PdNPs-6 biohybrid showed the same result (Table 4).

In summary, the straightforward *in situ* synthesis of metal NPs, induced by enzymes, generates new hybrid catalysts that could open a new way to rationally exploit the advantages offered by the combination of organometallic chemistry and biocatalysis.

This research was supported by The Spanish National Research Council (CSIC). Authors thank European Community (FP7-MULTIFUN) for the contract of M.M.

Notes and references

1 H. Häkkinen, *Nat. Chem.*, 2012, **4**, 443–455.
2 K. V. S. Ranganath, J. Kloesges, A. H. Schfer and F. Glorius, *Angew. Chem., Int. Ed.*, 2010, **49**, 7786–7789.
3 W. Sheng, Q. Yang and J. Weng, *Curr. Org. Chem.*, 2011, **15**, 3692–3705.
4 A. Fihri, M. Bouhrara, B. Nekoueishahraki, J.-M. Basset and V. Polshettiwar, *Chem. Soc. Rev.*, 2011, **40**, 5181–5203.
5 M.-C. Daniel and D. Astruc, *Chem. Rev.*, 2004, **104**, 293–346.
6 C.-L. Chen and N. L. Rosi, *Angew. Chem., Int. Ed.*, 2010, **49**, 1924–1942.
7 D. Ishii, K. Kinbara, Y. Ishida, N. Ishii, M. Okochi, M. Yohda and T. Aida, *Nature*, 2003, **423**, 628–632.
8 I. Willner, R. Baron and B. Willner, *Adv. Mater.*, 2006, **18**, 1109–1120.
9 J. Ge, J. Lei and R. N. Zare, *Nat. Nanotechnol.*, 2012, **7**, 428–432.
10 M. M. Bradford, *Anal. Biochem.*, 1976, **72**, 248–254.
11 (*a*) R. W. J. Scott, O. M. Wilson and R. M. Crooks, *J. Phys. Chem. B*, 2005, **109**, 692–704; (*b*) H. Li, J. K. Jo, L. D. Zhang, C.-S. Ha, H. Suh and I. Kim, *Langmuir*, 2010, **26**, 18442–18453.
12 (*a*) Y. T. Tan, J. Y. Lee and D. I. C. Wang, *J. Am. Chem. Soc.*, 2010, **132**, 5677–5686; (*b*) P. de la Presa, T. Rueda, M. del Puerto Morales, F. J. Chichon, R. Arranz, J. M. Valpuesta and A. Hernando, *J. Phys. Chem. B*, 2009, **113**, 3051–3057.
13 Z. Jin, M. Xiao, Z. Bao, P. Wang and J. Wang, *Angew. Chem., Int. Ed.*, 2012, **51**, 6406–6410.
14 (*a*) M. Nemanashi and R. Meijboom, *J. Colloid Interface Sci.*, 2013, **389**, 260–267; (*b*) J. Zhou and Q. Yang, *Chem.–Asian J.*, 2012, **7**, 2045–2050.
15 T. Jeffery, *Tetrahedron*, 1996, **52**, 10113–10130.
16 These values are comparable with the best ones reported in literature for this reaction in fully aqueous medium, see: F. Wang, C. H. Li, L.-D. Sun, C.-H. Xu, J. F. Wang, J. C. Yu and C.-H. Yan, *Angew. Chem., Int. Ed.*, 2012, **51**, 4872–4876.

